FREE ENERGY RELAXATION IN A DRIFT-TUBE LINAC

Nathan A. Brown, George H. Gillespie and Barrey W. Hill
G. H. Gillespie Associates, Inc., PO Box 2961, Del Mar, CA 92014

Abstract

A beam that is injected in a state that is not in equilibrium has free energy that can be thermalized as the density profile relaxes. Relaxation will also occur as the beam evolves through a channel with changes in energy, size and shape, and this relaxation will affect the subsequent beam behavior in the channel. PARMILA is used to simulate various input distributions for beams in a drift-tube linear accelerator. Properties of the final beam state, including size, shape, emittance and the presence of halo particles, are found for each of the initial phase space distributions.

1 INTRODUCTION

Charged particle beams are normally injected into focusing and accelerating channels with distributions in phase space that are not in thermal equilibrium [1, 2]. Any beam that is not in equilibrium has free energy that can be thermalized as relaxation occurs. Mismatch, misalignments and nonequilibrium density profiles are well-known sources of free energy that can be thermalized during relaxation [3]. The changes in the external forces that a beam experiences as it evolves through a series of lenses and accelerating sections also affect the relaxation process and can prevent the phase space distribution from coming close to equilibrium. Knowledge of the emittance growth resulting from the relaxation of free energy, and the rate at which it occurs, is important for applications requiring high intensity, low emittance beams, such as high energy colliders, spallation neutron sources, tritium production, radioactive waste transmutation, free electron lasers, and heavy ion inertial fusion.

Emittance growth resulting from space charge forces has been found analytically and with simulations for continuous beams [3-5] and for bunched beams [6]. Measurements of emittance growth from free energy have also been found to agree with simulations for a continuous beam in a periodic solenoid channel [7]. All of these cases considered beams with continuous focusing or with smooth periodic focusing.

PARMILA is used here to simulate a bunched proton beam through the first few cells of a drift-tube linear accelerator (DTL). Comparison is made between the final beam properties, including size, shape, emittance and the presence of a halo, for different initial distributions. The beam in each case experiences variations in eccentricity and size by factors of approximately two, so that in each case the relaxation of free energy, which affects the beam size and emittance, has subsequent effect on the evolution of the beam through the channel. Similar initial distributions, therefore, can have significantly different final beam sizes, shapes, density profiles and emittances.

The beam distributions are presented here with a new analysis tool in the graphic user interface (GUI) for PARMILA. This tool and the GUI are described in Section 2. In Section 3, variations in the final beam properties found with PARMILA are compared for several initial distributions, and comparison is made with previous results.

2 THE GRAPHIC USER INTERFACE

A graphic user interface has been developed for use with PARMILA in the Shell for Particle Accelerator Related Codes (S.P.A.R.C.) [8, 9]. Graphical icons represent beamline elements, and channel setup is accomplished by selecting and dragging the icons from a palette bar. Beam and channel parameters are controlled in an intuitive way through multi-pane windows connected with each element, so that a beamline can be set up and run with no knowledge of how to write a PARMILA input file.

As part of this GUI, we are developing an analysis tool that shows three-dimensional color plots of the particle distributions at any point along the channel. Each particle is represented by a point or a small sphere. These distributions can be rotated freely to allow the user to visually analyze the particle distributions in three dimensions. Figure 1 shows the final distribution for a bunched beam simulated with PARMILA through ten cells of a DTL. Changes in the density profiles, the shape and size of the beam, and the evolution of halo particles can be easily seen with this tool in conjunction with the GUI.

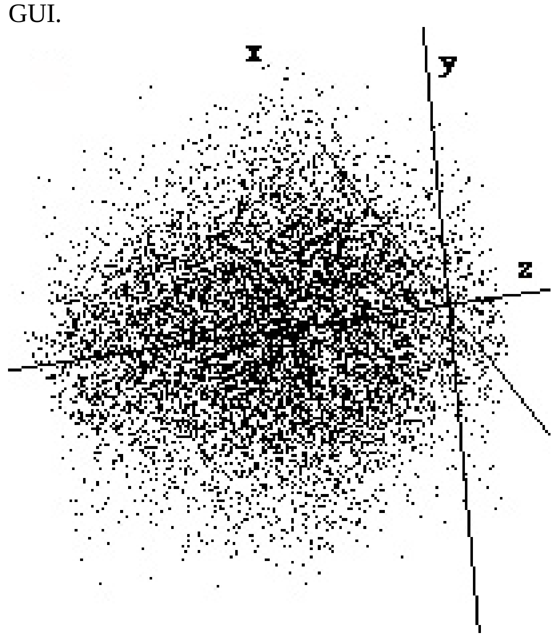

Figure 1: Final distribution of an initially uniform (ellipsoidal) beam after passing through ten cells of a DTL. Transverse halo particles are distributed approximately uniformly along the longitudinal direction.

0-7803-4376-X/98/$10.00 © 1998 IEEE

3 SIMULATION RESULTS

Six different initial density profiles were simulated with PARMILA in a 200 MHz DTL. The initial matched beam state has an average radius of 2.7 mm and a half-length of 5.4 mm. The initial beam was matched into the first lens of the DTL with variations in the transverse envelopes of +20% from the average in x and -20% from the average in y. The phase angle was -40^{o} in the rf wave, and the initial beam had a phase half-width of about 20^{o}. At the position of the final distribution, the beam has traveled through ten cells of the DTL from 2 MeV to 3 MeV, in a time of about one plasma period. In this distance, significant density profile relaxation and emittance growth has occurred in every case.

The six initial distributions were uniform ellipsoidal, Gaussian truncated at three standard deviations, Gaussian truncated at four standard deviations, parabolic, conical and a grid distribution. All of these distributions will experience different changes in self-potential energy and thermal energy if they are allowed to relax towards a thermal equilibrium density profile; in this channel, they experienced changes in shape and size along each dimension by factors of approximately two as the relaxation of free energy occurred. As a result of this, the beam evolution through the channel is different in every case. The final beam states have different density profiles, and they also developed different sizes and shapes as they reacted to the external focusing forces of the DTL. Three final beam profiles are shown in Figures 1, 2 and 3. All six initial distributions are included in Tables 1 and 2, which show the fractional changes in the emittance and rms size for each beam in the x, y and z directions.

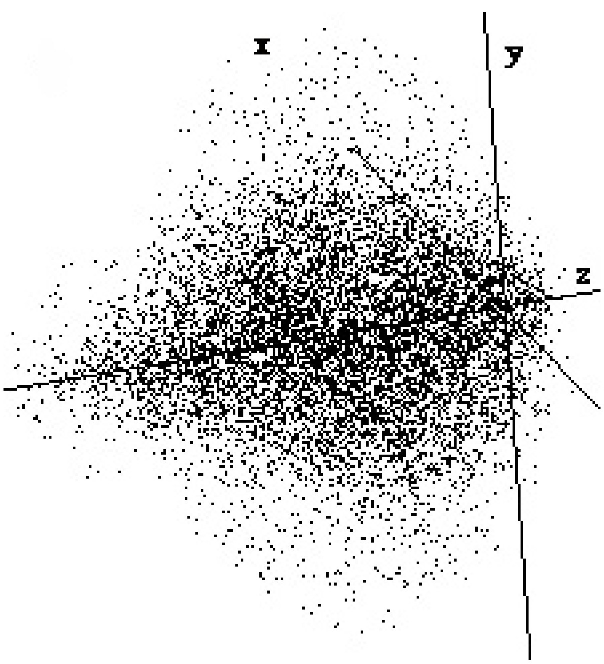

Figure 2: Final distribution of an initially Gaussian beam after passing through ten cells of a DTL. The halo particles are separated along the three focusing directions.

Figures 1, 2 and 3 show the final distributions in three dimensions for three different initial beam distributions in the same channel. In Figure 1 the initial density profile is uniform. Figure 2 shows a distribution for a beam that initially has a Gaussian density profile that is truncated at four rms radii, and Figure 3 corresponds to an initially parabolic profile.

The three-dimensional beam distribution in Figure 1 has a slight longitudinal tail in the trailing end of the bunch. This is also present in the profiles of Figures 2 and 3. This feature is also present in the thermal equilibrium distribution for a bunched beam with external focusing that is linear in the transverse direction and nonlinear in the longitudinal direction due to the shape of the effective focusing potential of the rf bucket [10]. The beams that start with a longitudinal tail (the initially Gaussian and parabolic profiles of Figures 2 and 3) have a more pronounced longitudinal tail in the trailing end than the initially uniform ellipsoidal beam.

The distribution shown in Figure 2 has a separation of the halo particles along the three focusing axes, and also has the largest emittance growth of the three shown, probably due to the initial state with particles at large distances from the beam center. The largest relative transverse halo of the three initial distributions shown is in the initially parabolic beam in Figure 3.

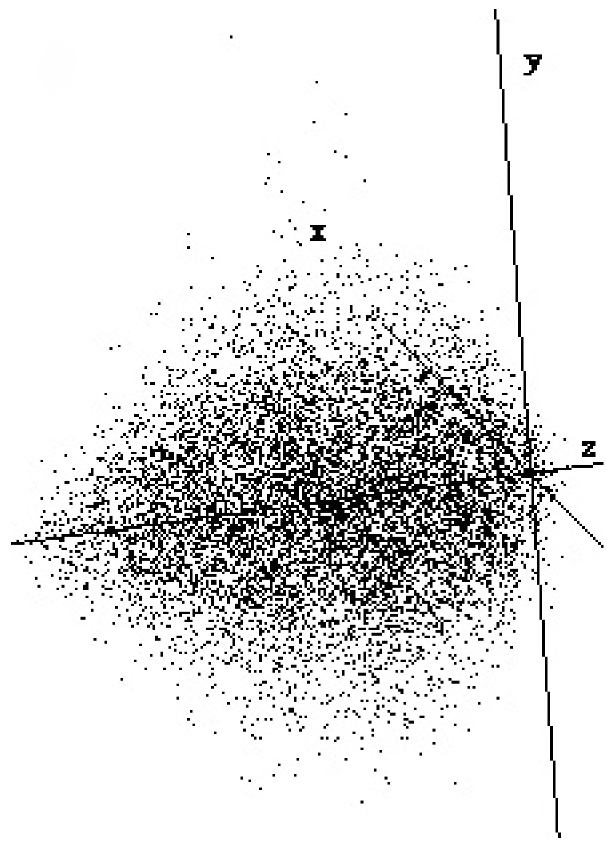

Figure 3: Final distribution of an initially parabolic beam after passing through ten cells of a DTL. The transverse halo near the longitudinal center of the beam is the largest of the three distributions shown, in comparison with the extent of the beam core.

Table 1: Ratios of final to initial rms emittance in the x, y, z directions at the end of ten cells in the DTL.

Initial State	$\varepsilon_{xf}/\varepsilon_{xi}$	$\varepsilon_{yf}/\varepsilon_{yi}$	$\varepsilon_{zf}/\varepsilon_{zi}$
Uniform	1.3	1.3	2.9
Gaussian3	2.2	2.4	4.1
Gaussian4	3.5	1.7	5.3
Parabolic	1.2	1.6	3.3
Conical	1.7	1.7	2.8
Grid	1.4	1.7	3.6

Table 1 shows the fractional changes in emittance for each of six initial distributions. The largest emittance increase in every case occurred along the longitudinal direction. This was probably due to nonlinearities in the longitudinal focusing, which are evident from the three-dimensional particle distributions of Figures 1, 2 and 3.

Table 2 shows the fractional changes in rms beam size for each of the six initial distributions. The initial beam entered the first quadrupole lens of the DTL with 20% variations in the x and y beam envelopes from the average beam envelope. The beam in each case was rms-matched into the DTL, and the relaxation of free energy then led to variations in the size of the oscillations in every direction and also to mismatch. The final beam state in every case had a larger fractional difference between the x and y rms sizes after traveling through ten cells. The largest fractional transverse emittance increases, however, varied in direction from one initial distribution to the other. Only for the intially Gaussian beam truncated at four standard deviations was the fractional x emittance increase larger than in y; for the others either the fractional y emittance increase was larger or there was not a significant difference.

4 CONCLUSION

Six different initial beam distributions were simulated with PARMILA through ten cells of a DTL. A significant amount of emittance growth from free energy was found to occur in the time of about one plasma period in all six cases. Variations in the final beam size between the different initial distributions were also found, showing the effects of the conversion of free energy on the evolution of the beam through the periodic channel.

In each of six cases, fractional changes in the rms emittance and beam size were shown in x, y and z. Although each beam started rms-matched in the same channel, the relaxation of free energy from the initial distributions affected the subsequent evolution so that there were large variations in the final rms beam properties.

The final three-dimensional beam distributions were shown for three cases, revealing variations in the beam distribution, including the presence of longitudinal tails and the extent and positions of halo particles.

A new graphical visualization tool for the PARMILA GUI has been described and used, and it has proven valuable in analyzing the beam distributions.

Table 2: Ratios of final to initial rms beam size in x, y and z directions at the end of ten cells in the DTL. The initial beam size was about 45% larger in x than in the y direction for matching into the first lens of the DTL.

Initial State	x_{mf}/x_{mi}	y_{mf}/y_{mi}	z_{mf}/z_{mi}
Uniform	1.2	1.1	1.5
Gaussian3	1.7	1.2	1.8
Gaussian4	2.2	1.0	1.6
Parabolic	1.5	1.1	1.7
Conical	1.7	1.3	1.8
Grid	0.9	0.7	3.5

5 REFERENCES

[1] M. Reiser and N. Brown, "Thermal Distribution of Relativistic Particle Beams with Space Charge," Phys. Rev. Lett. 71, 18, p2911 (1993).

[2] N. Brown and M. Reiser, "Thermal Equilibrium of Bunched Charged Particle Beams," Phys. Plasmas 2, 3, p965 (1995).

[3] M. Reiser, "Free energy and emittance growth in nonstationary charged particle beams," J. Appl. Phys. 70, 4, 1919 (1991).

[4] P. Lapostolle, "Possible Emittance Increase Through Filimentation due to Space Charge in Continuous Beams," IEEE Transactions on Nuclear Science, NS 18, p1101.

[5] T. Wangler, "Emittance Growth from Space Charge Forces," in High Brightness Beams for Advanced Accelerator Applications, College Park, MD, p21 (1991).

[6] I. Hofmann and J. Struckmeier, "Generalized Three Dimensional Equations for the Emittance and Field Energy of High-Current Beams in Periodic Focusing Structures," Part. Accel. 21, p69 (1987).

[7] I. Haber, D. Kehne, M. Reiser and H. Rudd, "Experimental, theoretical, and numerical investigation of the homogenization of density nonuniformities in the periodic transport if a space- charge dominated beam," Phys. Rev. A44, p5194 (1991).

[8] G. Gillespie, B. Hill and J. Gillespie, "Making PARMILA Easy to use - *Really Easy to Use!*," Proceedings of the 10th International Conference on High Power Particle Beams, San Diego, 1994, p626.

[9] G. Gillespie and B. Hill, "An Interactive Graphical User Interface for the Linac Beam Dynamics Code PARMILA," Proceedings of the 1994 International Linac Conference, Tsukuba, Japan, p517.

[10] N. Brown and M. Reiser, "Longitudinal current losses in rf linear accelerators," Phys. Rev. E54, p4188 (1996).